Surface passivation of n -type doped black silicon by atomic-layer-deposited SiO_2/Al_2O_3 stacks

van de Loo, B.W.H.; Ingenito, A.; Verheijen, M. A.; Isabella, O.; Zeman, M.; Kessels, W. M.M.

DOI
10.1063/1.4989824

Publication date
2017

Document Version
Final published version

Published in
Applied Physics Letters

Surface passivation of n-type doped black silicon by atomic-layer-deposited SiO_2/Al_2O_3 stacks

B. W. H. van de Loo, A. Ingenito, M. A. Verheijen, O. Isabella, M. Zeman, and W. M. M. Kessels

Citation: Appl. Phys. Lett. **110**, 263106 (2017); doi: 10.1063/1.4989824
View online: http://dx.doi.org/10.1063/1.4989824
View Table of Contents: http://aip.scitation.org/toc/apl/110/26
Published by the American Institute of Physics

Surface passivation of *n*-type doped black silicon by atomic-layer-deposited SiO_2/Al_2O_3 stacks

B. W. H. van de Loo,[1,a)] A. Ingenito,[2,a)] M. A. Verheijen,[1] O. Isabella,[2] M. Zeman,[2] and W. M. M. Kessels[1]

[1]*Department of Applied physics, Eindhoven University of Technology, P.O. Box 513, 5600 MB Eindhoven, The Netherlands*

[2]*Delft University of Technology, Department of Electrical Engineering, Mathematics and Computer Science, Mekelweg 4, 2628 CD Delft, The Netherlands*

(Received 7 April 2017; accepted 12 June 2017; published online 27 June 2017)

Black silicon (b-Si) nanotextures can significantly enhance the light absorption of crystalline silicon solar cells. Nevertheless, for a successful application of b-Si textures in industrially relevant solar cell architectures, it is imperative that charge-carrier recombination at particularly highly *n*-type doped black Si surfaces is further suppressed. In this work, this issue is addressed through systematically studying lowly and highly doped b-Si surfaces, which are passivated by atomic-layer-deposited Al_2O_3 films or SiO_2/Al_2O_3 stacks. In lowly doped b-Si textures, a very low surface recombination prefactor of 16 fA/cm^2 was found after surface passivation by Al_2O_3. The excellent passivation was achieved after a dedicated wet-chemical treatment prior to surface passivation, which removed structural defects which resided below the b-Si surface. On highly *n*-type doped b-Si, the SiO_2/Al_2O_3 stacks result in a considerable improvement in surface passivation compared to the Al_2O_3 single layers. The atomic-layer-deposited SiO_2/Al_2O_3 stacks therefore provide a low-temperature, industrially viable passivation method, enabling the application of highly *n*- type doped b-Si nanotextures in industrial silicon solar cells. *Published by AIP Publishing.*
[http://dx.doi.org/10.1063/1.4989824]

Black silicon (b-Si) nanotextures can strongly enhance the light absorption of industrial crystalline silicon (c-Si) solar cells. Specifically, b-Si nanotextures induce a high absorption over a wide wavelength range without the need for an anti-reflection coating (ARC),[1–4] even for light entering under wide range of angles.[2,5] The latter can increase the energy yield of solar cells operating under realistic, non-ideal conditions. Even for ultra-thin c-Si wafers with a thickness of $<35\ \mu$m, the light absorption can approach the fundamental classical absorption limit when the b-Si is combined with a back reflector.[5] Despite these outstanding optical properties of b-Si, numerous challenges still have to be overcome for realizing a large-scale breakthrough of b-Si in the field of photovoltaics. Most prominently, the b-Si should ideally become compatible with a heavily *n*-type doped Si front surface (in brief n^+ Si) which is typically used in solar cells. This should be realized without inducing significant additional surface recombination, although the large surface area and high roughness of b-Si surfaces render its passivation historically challenging.

Over the last decade, considerable progress has been made in the passivation of b-Si surfaces,[2,6–9] which has largely been enabled by Al_2O_3 films prepared by atomic layer deposition (ALD).[10,11] As ALD is based on self-limiting surface reactions, conformal deposition of thin films over b-Si textures can easily be achieved. Moreover, Al_2O_3 provides a very low interface defect density $Dit < 10^{11}\,\mathrm{eV^{-1}\,cm^{-2}}$, resulting in excellent *chemical* passivation, in combination with a distinctively high negative fixed-charge density Q_f in the range of $\sim 10^{12} - 10^{13}\,\mathrm{cm^{-2}}$.[12] The large negative Q_f brings the tips of the lowly doped b-Si needles in depletion or accumulation, resulting in high levels of *field-effect* passivation.[8] Due to this field-effect, very low surface recombination rates have been reported for lowly doped b-Si, even lower than what could expected on the basis of the large b-Si surface area.[6–8,13] As result, interdigitated back contact solar cells with a conversion efficiency of 22.1% have recently been demonstrated with the lowly *p*-type doped b-Si front surface being passivated by ALD Al_2O_3.[2]

Even though Al_2O_3 provides excellent passivation of lowly doped b-Si, standard industrially produced solar cell architectures, such as the aluminum back surface field (Al-BSF) cell and passivated emitter and rear cell (PERC), fundamentally rely on a heavily *n*-type doped Si front surface. Unfortunately, Al_2O_3 is not well suited for the passivation of these n^+ Si surfaces, as its high negative Q_f increases the minority charge carrier density which increases surface recombination.[14] Recently, stacks of thermally grown SiO_2 and PE-CVD SiN_x films have been explored as a passivation scheme for highly *n*-type-doped black Si surfaces.[15,16] Interestingly, ALD SiO_2/Al_2O_3 stacks have also emerged as an alternative passivation scheme for n^+ Si.[17] The ALD SiO_2/Al_2O_3 stacks do not exhibit a high negative Q_f, as a sufficiently thick SiO_2 layer prevents the injection of electrons from the c-Si bulk into the Al_2O_3.[18] Moreover, the stack provides excellent levels of chemical passivation with $D_{it} < 10^{11}\,\mathrm{eV^{-1}\,cm^{-2}}$; it can be deposited at low temperatures and with a high conformality over surfaces with high roughness.[19,20] Therefore, the ALD SiO_2/Al_2O_3 stack is an interesting candidate for the surface passivation of n^+-type b-Si nanotextures.

[a)]B. W. H. van de Loo and A. Ingenito contributed equally to this work.

In this letter, carrier-recombination at lowly doped and highly doped *n*-type b-Si is addressed. b-Si nanotextures have been created using reactive ion- etching, followed by short alkaline etch steps, termed the "defect removal etch," (DRE) to control the b-Si surface morphology.[15] The b-Si surfaces are passivated by ALD Al_2O_3 and SiO_2/Al_2O_3 stacks. First, the morphological and optical properties of b-Si surfaces are studied. Second, the surface passivation of lowly doped b-Si surfaces is addressed as a starting point, before considering the passivation of b-Si which has been additionally *n*-type doped through ion implantation of phosphorus. Finally, the potential of highly n^+-type doped b-Si passivated by SiO_2/Al_2O_3 for applications as front surface texture in c-Si solar cells is revealed through corona-charging experiments.

Lifetime samples with a b-Si front surface were created by RIE of planar 280–μm thick floatzone Si (100) wafers (*n*-type, 2.8 Ω cm) using a SF6 and O_2 plasma in a Drytek Triode 384T Plasma Etcher at room temperature. The samples were subjected to diluted Tetramethylammonium hydroxide (1%) for 0, 15, or 30 s to remove structural defects, following the approach of Ingenito *et al.*[15] Subsequently, two groups of b-Si front surfaces were heavily *n*-type doped using phosphorus ion implantation with constant energy (20 keV) and variable doses of 5×10^{14} cm^{-2} (termed "low dose") and 1×10^{15} cm^{-2} (termed "high dose"). This was followed by annealing at 850 °C for 90 min in O_2 ambient and a buffered hydrofluoric acid (BHF) etch.

The polished rear sides of the lifetime samples were passivated by 30-nm thick Al_2O_3 layers, whereas the b-Si front surfaces were passivated by either a single Al_2O_3 layer or by SiO_2/Al_2O_3 stacks. The Al_2O_3 was prepared using 272 consecutive ALD cycles of 60 ms exposure to $Al(CH_3)_3$, a 3.5 s purge, 4 s O_2 plasma, and a 0.5 s purge in an Oxford Instruments OpAL^{TM} reactor at 200 °C, yielding a constant growth rate of 1.1 Å/cycle. The SiO_2 was deposited in 33 ALD cycles at the same temperature in the abovementioned reactor. The SiO_2 ALD cycles consist of a 250 ms exposure to $H_2Si(N(C_2H_5)_2)_2$, a 3.5 s purge, a 5 s O_2 plasma step, and a 1 s purge, yielding (after the formation of an ultra-thin oxide) a steady-state growth of 0.9 Å/cycle, as was verified on planar wafers by spectroscopic ellipsometry. Note that a SiO_2 thickness of 4–5 nm has proven to be sufficient for optimized passivation of n^+ Si in previous work.[17] Immediately after deposition of SiO_2, the Al_2O_3 capping layer was deposited without vacuum break. Next, the samples received a postdeposition anneal at 400 °C in N_2 ambient for 10 min.

The absorption of the samples was derived from $1 - R - T$, where the wavelength-dependent reflectance (R) and transmittance (T) were measured using an integrating-sphere PerkinElmer Lamda 950 spectrophotometer. The doping of the b-Si samples has been characterized by evaluating the sheet resistance by the four-point probe. Lifetime measurements were carried out using quasi-steady-state photoconductance (QSSPC) measurements in a Sinton WCT100. The implied open-circuit voltage was derived under 1-sun illumination (iV_{oc}), whereas the recombination parameter J_0 was derived from QSSPC using the method of Kane and Swanson.[21] Note that the J_0 could not in all cases be reliably extracted using this method. In these cases, J_0 was therefore determined from the iV_{oc}. On selected samples, corona charges were deposited on the b-Si by applying a voltage of 11 kV between the sample and a tungsten needle for 25 min.

Figure 1 shows the scanning- and high-resolution transmission electron microscopy (SEM and TEM) images of the passivated b-Si surfaces. The detailed TEM analysis of a b-Si nanopillar in Fig. 1(c) reveals the presence of structural damage at the tips of the needles for the sample that has not have been subjected to the DRE. The presence of defects can be attributed to ion bombardment during the room-temperature RIE process. In other studies addressing the preparation of b-Si by RIE, such defects were not reported,[8] potentially due to the more gentle structuring of the b-Si surface by RIE at cryogenic temperatures as opposed to the room temperature RIE which was carried out in this work. Note however, that processing at room temperatures is highly desirable for high-volume manufacturing.

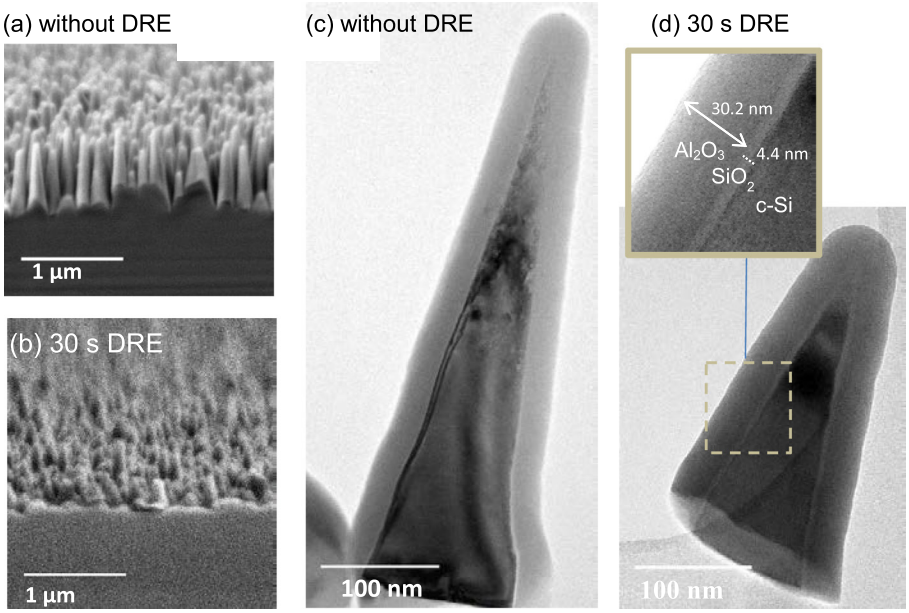

FIG. 1. Cross-sectional scanning electron microscopy (SEM) images of b-Si surfaces (a) without or (b) with 30 s of defect removal etching (DRE). (c) Transmission electron microscopy (TEM) images of a b-Si needle without DRE passivated by 30-nm thick ALD Al_2O_3. (d) TEM of a b-Si needle with 30 s of DRE passivated by ALD SiO_2/Al_2O_3. In the inset, the film thicknesses are indicated.

Figure 1(d) shows a b-Si needle which was exposed to 30 s of DRE. Interestingly, most of the region containing the defects has been etched away during DRE, indicating that these defects were apparently confined to a sub-surface region. With increasing DRE time, the roughness of the b-Si decreases [see Figs. 1(a) and 1(b)]. For all b-Si nanotextures evaluated in this work, Al_2O_3 layers or SiO_2/Al_2O_3 stacks could be grown conformally over the pillars, see e.g., Figs. 1(c) and 2(d).

In Fig. 2(a), the absorbance of passivated b-Si samples is compared to the current industrial standard texture of monocrystalline silicon, i.e., a random-pyramid (RP) texture combined with a 75-nm thick SiN_x anti-reflection coating. The sharp features of the b-Si texture gradually change the refractive index of air into that of Si, which minimizes front reflection. Especially in the ultra-violet region (300–500 nm), b-Si textures therefore show a significant higher absorption than the RP-texture. However, because of the small size of the nanotextured features, the scattering of long wavelength light (1000–1100 nm) is weaker than that for a RP texture. It has been shown elsewhere that the absorption in this range can be increased by combining the b-Si with a microtextured rear surface[5] or by superimposing b-Si on a RP-textured front surface.[15]

In Fig. 2(b), the impact of the DRE time on the optical properties of the b-Si surfaces is shown. As the figure depicts, for DRE times of 30 s or longer, the absorbance of b-Si is reduced over the entire wavelength range, which can

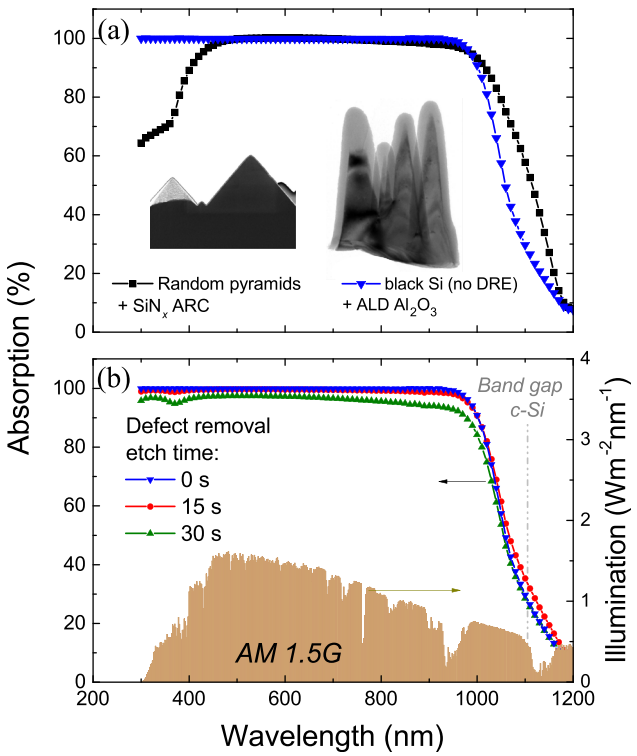

FIG. 2. (a) Absorption in 280 μm thick c-Si with either a b-Si front surface texture which was passivated by 30 nm of ALD Al_2O_3 or a random-pyramid texture and a 75-nm SiN_x anti-reflection coating. The inset shows scanning and transmission electron microscopy images of the surface textures (not to scale). (b) Absorption of b-Si, passivated by 30 nm of Al_2O_3, for various defect removal etching (DRE) times. Additionally, the AM1.5 spectrum is displayed for reference.

be attributed to the reduced surface roughness of the b-Si textures [Fig. 1(b)].

In Table I, lifetime results are given for various passivated b-Si lifetime samples. First, b-Si textures which were not subjected to ion-implantation are assessed to determine the b-Si quality. In case the b-Si texture was not subjected to DRE, and thus contained sub-surface defects, the samples could already be passivated reasonably well by Al_2O_3 single layers, resulting in $J_0 = 47$ fA/cm^2 and $iV_{oc} = 685$ mV. Yet, when applying the DRE, the total J_0 for b-Si passivated by Al_2O_3 improves considerably down to 24 and 16 fA/cm^2 for 15 and 30 s of etching, respectively (see Table I), resulting in high iV_{oc} values to well above > 690 mV. This improvement can be attributed to a reduced surface area and to the removal of structural defects. Note that for short etch times of 15 s, the recombination was reduced without compromising the outstanding optical properties [see Fig. 2(b)].

Note, that it is often postulated that surface passivation of b-Si by Al_2O_3 is highly dependent on the strong field-effect passivation on such lowly doped samples provided by the large negative Q_f of Al_2O_3.[6,8] Indeed, when passivating the b-Si by SiO_2/Al_2O_3 stacks (which do not exhibit the strong negative Q_f and accompanied field-effect passivation), the recombination is considerably higher, resulting in a low iV_{oc} of 589 mV, further underlining that field-effect passivation is truly playing a significant role in the passivation of b-Si surface textures.

As a next step, highly n-type doped b-Si surfaces which received a phosphorus ion-implantation dose were considered. Remarkably, the sheet resistance of the b-Si samples was found to be significantly higher that than for planar surfaces which received the same ion implantation dose (i.e., above $> 80\,\Omega$/sq for the low dose and $> 62\,\Omega$/sq for the high dose for b-Si, compared to 57 Ω/sq and 38 Ω/sq for planar surfaces, respectively). The higher sheet resistances for b-Si can be explained as the phosphorus dopants within the tip of the needles do not contribute significantly to the lateral conduction. Therefore, significant ion-implantation doses were required on b-Si to achieve a relatively low sheet resistance. Note that also for ion implantation by boron, b-Si surfaces have resulted considerably higher sheet resistances compared to planar surfaces.[9]

As is shown in Table I, the surface passivation of the n^+-type b-Si surfaces by Al_2O_3 for a low or high ion implantation dose resulted in iV_{oc} values below 611 mV, for all DRE times used. The poor passivation of n^+ Si by Al_2O_3 was, as was stated in the introduction, expected on the bases of its large negative Q_f which increases the minority carrier density at these surfaces. Indeed, when using SiO_2/Al_2O_3 stacks considerably higher iV_{oc} values were achieved, as the SiO_2/Al_2O_3 do not exhibit such negative Q_f. Moreover, the passivation of n^+ b-Si by SiO_2/Al_2O_3 improved significantly by application of the DRE. The highest iV_{oc} value obtained for n^+-type b-Si is 641 mV.

To assess whether the surface passivation of this best case could be further improved, positive corona charging was carried out. Due to added positive charges, the field-effect passivation was enhanced, and the iV_{oc} saturated at 652 mV after prolonged charging. This final iV_{oc} is 11 mV higher than before corona charging. Therefore, the iV_{oc} of the n-type

TABLE I. Lifetime results of b-Si samples (*n*-type, 3 Ω cm) etched with various defect removal etching times and subjected to several phosphorus ion implantation doses. The b-Si textured surface was passivated either by ALD Al_2O_3 or by ALD SiO_2/Al_2O_3 stacks, whereas the polished rear surface was passivated by ALD Al_2O_3 in all cases.

			Al_2O_3 passivation		SiO_2/Al_2O_3 passivation	
Ion implantation	DRE time (s)	R_{sheet} (Ω/sq)	iV_{oc} (mV)	J_0 (fA/cm^2)	iV_{oc} (mV)	J_0 (fA/cm^2)
No dose	0	>100	685	47	589	2530
	15	>100	695	24	590	1850
	30	>100	692	16	603	1580
Low dose (5×10^{14} cm^{-2})	0	86 ± 3	589	700	625	639
	15	80 ± 1	599	628	629	524
	30	81 ± 2	600	750	639	338
High dose (10^{15} cm^{-2})	0	71 ± 2	596	541	620	843
	15	64 ± 2	611	644	641[a]	312[a]
	30	62 ± 2	609	719	640	300

[a]Used for corona charging.

doped b-Si sample could only marginally be improved by increased (field-effect) passivation, from which it can be expected that the iV_{oc} is not limited by surface recombination but, e.g., by Auger recombination in the b-Si. Presumably, the high phosphorus ion-implantation doses which were required to achieve the low sheet resistances in the b-Si resulted in significant Auger recombination. In future studies, deeper and lower *n*-type doped regions could therefore be a promising approach to further improve the iV_{oc}. For instance, if dopants do not reside within the tips of the b-Si needles, they can contribute to the lateral conduction of charge carriers, and lower ion-implantation doses can be used. Moreover, lower doping concentrations will induce less Auger recombination.

In conclusion, in this work, ALD SiO_2/Al_2O_3 stacks have been evaluated as a low-temperature passivation scheme for highly *n*-type doped b-Si nanotextures prepared by room-temperature RIE. TEM investigations revealed structural defects which reside below the b-Si surface but which could be removed through a brief DRE without significantly affecting the excellent light in-coupling properties of b-Si. In this way, lowly doped b-Si passivated by ALD Al_2O_3 resulted in low recombination as is evident by $J_0 = 16$ fA/cm^2 and $iV_{oc} = 695$ mV. For n^+-type b-Si which was more heavily *n*-type doped through ion implantation of phosphorus, a combination of DRE and the use of ALD SiO_2/Al_2O_3 passivation stacks resulted in significantly reduced surface recombination compared to ALD Al_2O_3 and $iV_{oc} = 641$ mV, providing a first step towards the application of highly *n*-type doped b-Si nanotextures in silicon solar cells.

The authors gratefully acknowledge R. H. J. Vervuurt and C. A. A. van Helvoirt for experimental assistance. This work was supported by the Dutch Ministry of Economic Affairs via the Top Consortia for Knowledge and Innovation (TKI) programs *Advanced Nanolayers* and *IBChampion*. The Solliance consortium and the Dutch province of Noord-Brabant are acknowledged for funding the TEM facility.

[1]W.-C. Wang, C.-W. Lin, H.-J. Chen, C.-W. Chang, J.-J. Huang, M.-J. Yang, B. Tjahjono, J.-J. Huang, W.-C. Hsu, and M.-J. Chen, ACS Appl. Mater. Interfaces **5**, 9752 (2013).
[2]H. Savin, P. Repo, G. von Gastrow, P. Ortega, E. Calle, M. Garín, and R. Alcubilla, Nat. Nanotechnol. **10**, 624 (2015).
[3]M. Gaudig, J. Hirsch, T. Schneider, A. N. Sprafke, J. Ziegler, N. Bernhard, and R. B. Wehrspohn, J. Vac. Sci. Technol., A **33**, 05E132 (2015).
[4]X. Liu, P. R. Coxon, M. Peters, B. Hoex, J. M. Cole, and D. J. Fray, Energy Environ. Sci. **7**, 3223 (2014).
[5]A. Ingenito, O. Isabella, and M. Zeman, ACS Photonics **1**, 270 (2014).
[6]P. Repo, A. Haarahiltunen, L. Sainiemi, M. Yli-Koski, H. Talvitie, M. C. Schubert, and H. Savin, IEEE J. Photovoltaics **3**, 90 (2013).
[7]M. Otto, M. Kroll, T. Käsebier, R. Salzer, A. Tünnermann, and R. B. Wehrspohn, Appl. Phys. Lett. **100**, 191603 (2012).
[8]G. von Gastrow, R. Alcubilla, P. Ortega, M. Yli-Koski, S. Conesa-Boj, A. Fontcuberta i Morral, and H. Savin, Sol. Energy Mater. Sol. Cells **142**, 29 (2015).
[9]G. von Gastrow, P. Ortega, R. Alcubilla, S. Husein, T. Nietzold, M. Bertoni, and H. Savin, J. Appl. Phys. **121**, 185706 (2017).
[10]G. Agostinelli, A. Delabie, P. Vitanov, Z. Alexieva, H. F. W. Dekkers, S. De Wolf, and G. Beaucarne, Sol. Energy Mater. Sol. Cells **90**, 3438 (2006).
[11]B. Hoex, S. B. S. Heil, E. Langereis, M. C. M. Van De Sanden, and W. M. M. Kessels, Appl. Phys. Lett. **89**, 42112 (2006).
[12]G. Dingemans and W. M. M. Kessels, J. Vac. Sci. Technol. A **30**, 40802 (2012).
[13]T. Allen, J. Bullock, A. Cuevas, S. Baker-finch, and F. Karouta, *Proceedings 40th IEEE Photovoltaic Specialist conference*, pp. 562–566.
[14]B. Hoex, M. C. M. van de Sanden, J. Schmidt, R. Brendel, and W. M. M. Kessels, Phys. Status Solidi RRL **6**, 4 (2012).
[15]A. Ingenito, O. Isabella, and M. Zeman, Prog. Photovoltaics Res. Appl. **23**, 1649 (2015).
[16]P. Li, Y. Wei, X. Tan, X. Li, Y. Wang, Z. Zhao, Z. Yuan, and A. Liu, RSC Adv. **6**, 104073 (2016).
[17]B. W. H. van de Loo, H. C. M. Knoops, G. Dingemans, G. J. M. Janssen, M. W. P. E. Lamers, I. G. Romijn, A. W. Weeber, and W. M. M. Kessels, Sol. Energy Mater. Sol. Cells **143**, 450 (2015).
[18]N. M. Terlinden, G. Dingemans, V. Vandalon, R. H. E. C. Bosch, and W. M. M. Kessels, J. Appl. Phys. **115**, 33708 (2014).
[19]G. Dingemans, N. M. Terlinden, M. A. Verheijen, M. C. M. van de Sanden, and W. M. M. Kessels, J. Appl. Phys. **110**, 93715 (2011).
[20]G. Dingemans, C. A. A. van Helvoirt, D. Pierreux, W. Keuning, and W. M. M. Kessels, J. Electrochem. Soc. **159**, H277 (2012).
[21]D. E. Kane and R. M. Swanson, in *18th IEEE Photovoltaic Specialists Conference* (IEEE, New York, 1985), pp. 578–583.